Investigation on the reflection and transmission properties of complex absorbing potentials

U. V. Riss and H.-D. Meyer
Theoretische Chemie, Physikalisch-Chemisches Institut, Universität Heidelberg, Im Neuenheimer Feld 253, 69120 Heidelberg, Germany

(Received 18 March 1996; accepted 18 April 1996)

The reflection and transmission properties of different complex absorbing potentials (CAPs) are studied using WKB and scaling procedures which make the results transferable to any mass and kinetic energy. Explicit formulas are obtained which describe the reflection and transmission properties of monomial CAPs $-i\eta x^n$ with high accuracy. These properties are now well understood. The approximate results are compared to exact analytical results available for quadratic CAPs, and to numerical results obtained by wave packet propagation followed by an energy resolved analysis. The approximate, but accurate, description of the action of the CAP is finally used to determine optimal CAP parameters. CAP length, strength, and order can now be chosen in such a way that the sum of reflection and transmission is minimized. Optimal parameters are compiled for different energies and energy intervals. © *1996 American Institute of Physics*. [S0021-9606(96)01628-5]

I. INTRODUCTION

Complex absorbing potentials (CAP) have gained increasing importance in the field of time-dependent[1,2] scattering theory since they were introduced to avoid artificial boundary reflections in finite grid or basis set calculations.[3] But also in the time-independent theory CAPs have successfully been applied.[4–6] Naturally a CAP does not serve as a panacea since it itself produces artificial reflections. Investigations of the reflection and transmission properties of CAPs are therefore, an important aspect for their applicability and a simple description of these features is a necessary tool for every practitioner applying CAPs.

The first attempts to describe reasonable conditions for CAPs lead back to Neuhauser and Baer[1] who for the first time successfully used CAPs to solve realistic scattering problems. More rigorous investigations on the determination of optimal parameters were performed by Child.[7] A thorough investigation on this point was carried out by Vibók and Balint-Kurti[8,9] and in these studies scaling procedures were introduced. Another extensive study on the optimization of absorbing potentials was performed by Macías, Brouard, and Muga[10] who compared different types of potential forms and optimized the various parameters. We will also refer to results of Seideman and Miller,[11] who used WKB methods for the description of absorption and reflection properties of CAPs. Although there have been several attempts to determine the absorption behavior of CAPs, the numerical investigations were such that easy-to-use formulas are still to be produced. These are not only necessary to derive optimal CAP parameters, but also to understand the essential structure of CAP absorption.

The starting point of the present work was the attempt to reproduce the numerical results of Vibók and Balint-Kurti[9] by applying a novel technique including flux operators,[12] which leads to a properly energy resolved description of the reflection and transmission. To this end a Gaussian wave packet is scattered off the CAP under investigation. The propagation of the wave packet is performed solving the time-dependent Schrödinger equation by application of the pseudo-spectral Newton method[13–15] and the fast Fourier transform (FFT) technique of Kosloff and Kosloff.[16] The flux into the reflection and the transmission channel is determined by additional boundary CAPs. This procedure yields an energy resolved analysis of the reflection and transmission properties.

Unfortunately, we failed in reproducing the numerical results of Ref. 9, such that we began to search for the reasons. Using simple scaling and WKB arguments, we have examined the essential features of the CAP absorption. The comprehension of the transmission by a direct WKB approach appears to be straightforward, while the description of the reflection is found to be more sophisticated. Here, we can refer to exact analytical results derived for the quadratic CAP in a previous paper.[17] The comparison to these results gives the decisive hint how to handle the reflection.

In Sec. II, we will present the theoretical methods which are used to determine the absorption parameters; in particular a scaling procedure is applied to the Schrödinger equation. Conclusions are then drawn for the description of reflection and transmission as functions of the CAP parameters and, furthermore, WKB considerations are applied to the problem. The formulas obtained are then used to derive equations for optimal CAP parameters. Except for some general considerations monomial CAPs $-i\eta x^n$ are exclusively investigated. In Sec. III, we will sketch the procedure applied to the numerical computation of energy resolved absorption parameters. In Sec. IV, we will present the numerical results and compare them to the formulas derived. In Sec. V, we will give a short discussion of the results and a comparison to the calculations of Vibók and Balint-Kurti.[9]

II. THEORY

A. Scaling behavior

Let us consider the one-dimensional time-independent Schrödinger equation

$$-\frac{\hbar^2}{2m}\frac{d^2\psi(x)}{dx^2}+[-i\eta W(x)-E]\psi(x)=0, \tag{2.1}$$

where E denotes a real energy, m the mass, and $-i\eta W(x)$ a usual CAP of finite length L located on the interval $[0,L]$. The reflection and transmission coefficients, $\mathscr{R}$ and $\mathscr{T}$, respectively, can be determined from the solution ψ. Outside the CAP this wave function must satisfy the boundary conditions:

$$\psi(x)=e^{ikx}+\mathscr{R}\cdot e^{-ikx} \quad \text{for } x<0, \tag{2.2a}$$

$$\psi(x)=\mathscr{T}\cdot e^{ikx} \quad \text{for } x>L, \tag{2.2b}$$

where $k=\sqrt{2mE/\hbar^2}$ denotes the (real) wave number. We introduce a parametrization similar to that described in Refs. 8 and 9:

$$\xi=\frac{x}{L}, \quad W_0(\xi)=\frac{W(\xi\cdot L)}{W(L)} \tag{2.3}$$

for $\xi\in[0,1]$. This leads to the parametrized equation

$$\frac{1}{k^2L^2}\frac{d^2\psi(\xi)}{d\xi^2}+\left[i\frac{\eta W(L)}{E}W_0(\xi)+1\right]\psi(\xi)=0, \tag{2.4}$$

which allows a reduction of the number of parameters. The advantage of this parametrization consists in the fact that only two parameters are left to be varied, namely

$$a=\frac{\eta W(L)}{E} \quad \text{and} \quad b=kL. \tag{2.5}$$

This way we obtain the following standardized differential equation:

$$\frac{d^2\psi(\xi)}{d\xi^2}+[b^2+iab^2W_0(\xi)]\psi(\xi)=0, \tag{2.6}$$

which only depends on a, b, and $W_0(\xi)$.

In the case of a monomial CAP of order n, i.e., $W(x)=x^n$, further simplifications are possible. In the following we will restrict the study to this, the most commonly used, class of CAPs which can be understood to a greater extent. For monomial CAPs we can use the transformation $\zeta=b\xi=kx$, which leads to a further reduction, yielding the differential equation

$$\frac{d^2\psi(\zeta)}{d\zeta^2}+(1+ic\zeta^n)\psi(\zeta)=0, \tag{2.7}$$

where

$$c=\frac{a}{b^n}=\frac{\eta}{Ek^n}, \tag{2.8}$$

and $\zeta\in[0,1/b]$. This parametrization will be shown to be suitable for the description of reflections from monomial CAPs.

B. Transmission

Semiclassical WKB approximations have proved to be very useful in the description of reflection and transmission properties of CAPs.[8,11,17,18] To calculate the transmission one may approximate the solution $\psi(x)$ of the Schrödinger Eq. (2.1) by

$$\psi(x)=\exp\left[\frac{i}{\hbar}\int_0^x\sqrt{2mE+2im\eta W(x')}dx'\right] \tag{2.9}$$

for $0\leqslant x\leqslant L$. As an approximate solution of Eq. (2.6) this function reads

$$\psi(\xi)=\exp\left[ib\int_0^\xi\sqrt{1+iaW_0(\xi')}d\xi'\right] \tag{2.10}$$

for $0\leqslant\xi\leqslant1$. The absorption is described by the damping of the wave function, while penetrating the CAP. This damping determines the transmission as

$$|\mathscr{T}|^2=|\psi(\xi=1)|^2 =\exp\left(-2b\ \mathrm{Im}\int_0^1\sqrt{1+iaW_0(\xi')}d\xi'\right). \tag{2.11}$$

Although it is possible to evaluate this expression numerically easier-to-use formulas are desirable. To this end we introduce the function $g(a)$ which reads

$$g(a):=\frac{2}{n+1}\ \mathrm{Im}\int_0^1\sqrt{1+iaW_0(\xi)}d\xi. \tag{2.12}$$

This leads to the following simple expression for the transmission:

$$|\mathscr{T}|^2=\exp\left(-\frac{g(a)b}{n+1}\right). \tag{2.13}$$

If we consider the case $a<1$, i.e., small η or high energies, an expansion of the square root in Eq. (2.12) is possible. Using the abbreviation

$$I_j:=\int_0^1 W_0(\xi)^j d\xi, \tag{2.14}$$

one obtains the following expansion for $g(a)$:

$$g(a):=\sum_{k=0}^{\infty}(-1)^j\binom{1/2}{2j+1}I_{2j+1}a^{2j+1} =a\left[1-\frac{n+1}{8(3n+1)}a^2+\frac{7(n+1)}{256(5n+1)}a^4-\cdots\right], \tag{2.15}$$

where the second line is only valid for monomial CAPs of order n. For $a\ll1$ the identification $g(a)\equiv a$ yields a useful approximation such that the transmission can be described by

$$|\mathscr{T}|^2=\exp\left(-\frac{ab}{n+1}\right). \tag{2.16}$$

For more accurate approximations of $g(a)$ we have to consider higher orders in the expansion Eq. (2.15) as well as the asymptotic behavior for $a\to\infty$. The latter can be directly

obtained from Eq. (2.11) neglecting the 1 under the square root. For the monomial case the asymptotics yield

$$g(a)=\frac{2n+2}{n+2}\sqrt{2a}+\cdots \quad \text{for } a\to\infty. \tag{2.17}$$

A useful approximation for $g(a)$ is given by

$$g(a)=a\cdot\left\{1+\frac{n+1}{3n+1}a^2+\frac{1}{16}\left(\frac{n+2}{2n+2}\right)^8 a^4\right\}^{-1/8}, \tag{2.18}$$

which is identical up to third order in a to the expansion (2.15) and obeys the asymptotics (2.17). In a similar way it is possible to approximate the inverse function of $g(a)$ by

$$a(g)=g\left\{1+\frac{n+1}{6n+2}g^2+\frac{1}{16}\left(\frac{n+2}{2n+2}\right)^8 g^4\right\}^{1/4}. \tag{2.19}$$

This inverse can be used to determine values for a if only $g(a)$ is known. We will use this formula later for the optimization of a. Note that $g(a)$ and $a(g)$ as given by Eqs. (2.18) and (2.19) are not strictly inverses of each other. They are, however, excellent approximations to the exact $g(a)$ defined by Eq. (2.15) and to its inverse $a(g)$, respectively.

C. Reflection

The reflection is more subtle than the transmission. One assumption which simplifies the consideration is that of infinite CAP length. This assumption appears to be legitimate since the effects of the finite CAP length only become important for high energies where, as shown by our numerical investigations, the transmission is already predominant. Assuming therefore an infinite CAP length, the solution of Eq. (2.7) depends only on the parameter $c:=a/b^n$. The wave function, and hence the reflection, are functions of this single parameter

$$\mathscr{R}(c)=\mathscr{R}\left(\frac{\eta}{Ek^n}\right). \tag{2.20}$$

This reflection coefficient can be calculated by matching the free solution for $x<0$ [see Eq. (2.2)] to the exact solution. Therefore, we have to consider the logarithmic derivative of $\psi(x)$ at $x=0$ and define

$$\mathscr{\ell}(c)\equiv\mathscr{\ell}(E,\eta):=ik\frac{\psi(x)}{\psi'(x)}\bigg|_{x=0}=i\frac{\psi(\zeta)}{\psi'(\zeta)}\bigg|_{\zeta=0}. \tag{2.21}$$

The matching yields

$$\mathscr{R}=\frac{\mathscr{\ell}(c)-1}{\mathscr{\ell}(c)+1}. \tag{2.22}$$

The determination of the function $\mathscr{\ell}(c)$ is in general a complicated task. A simple WKB approach fails. A hint as to what the function $\mathscr{\ell}(c)$ may look like can be obtained from the *exact* analytic result worked out for the quadratic CAP $-i\eta x^2$ in Ref. 17. One finds that

$$\mathscr{\ell}(c)=-i\tan\left[\pi\left(\sqrt{\frac{i}{16c}}+\frac{1}{4}\right)\right]f(c), \tag{2.23}$$

where

$$f(c)=\sqrt[4]{\frac{i}{16c}}\frac{\Gamma\left(\sqrt{\frac{i}{16c}}+\frac{1}{4}\right)}{\Gamma\left(\sqrt{\frac{i}{16c}}+\frac{3}{4}\right)}=1+\frac{i}{4}c-\frac{21}{32}c^2+\cdots. \tag{2.24}$$

In this expression for $\mathscr{\ell}(c)$, we have to distinguish two factors: the tangent factor, which is essentially singular for $c\to0$, and the residual factor f, which can asymptotically be expanded in orders of c.

In order to calculate $\mathscr{\ell}(c)$, one has to determine the wave function and its derivative at $x=0$. Since these are determined subject to the boundary condition $\psi(x)\to0$ for $x\to\infty$ (assuming an infinite CAP length), an approximation for the wave function is required that is uniformly accurate on the interval $[0,\infty)$. Since the CAP is unbounded, one is faced with a turning point problem that can be solved by incorporation of the Airy function,[19] yielding an uniform WKB approximation.[20,21] Moreover, higher order CAPs require higher order WKB approaches. The details are given in Appendix A. Here we only note, that the (reciprocal) logarithmic derivative $\mathscr{\ell}(c)$ can be written in complete agreement with Eq. (2.23) as

$$\mathscr{\ell}(c)=-i\tan\left(\beta_n(i/c)^{1/n}+\frac{\pi}{4}\right)f(c), \tag{2.25}$$

where we found it sufficient to determine f to first order in c, i.e.,

$$f(c)=1+2\alpha_n c. \tag{2.26}$$

The coefficients α_n and β_n are given by

$$\alpha_n=\frac{n!}{4i}\left(\frac{i}{2}\right)^n, \tag{2.27}$$

and

$$\beta_n=\frac{\Gamma(1+1/n)\Gamma(3/2)}{\Gamma(1/n+3/2)}. \tag{2.28}$$

For the convenience of the reader we compile: $\alpha_1=1/8$, $\alpha_2=i/8$, $\alpha_3=-3/16$, $\alpha_4=-3i/8$ and $\beta_1=2/3$, $\beta_2=\pi/4$, $\beta_3=0.841\,309$, $\beta_4=0.874\,019$.

From Eqs. (2.22) and (2.25) results the following expression for the reflection:

$$|\mathscr{R}|^2=\left|\frac{\frac{f(c)-1}{f(c)+1}-\exp\{2i[\beta_n(i/c)^{1/n}+\pi/4]\}}{1-\frac{f(c)-1}{f(c)+1}\exp\{2i[\beta_n(i/c)^{1/n}+\pi/4]\}}\right|^2. \tag{2.29}$$

As we shall see below this simple formula is remarkably accurate.

The tangent term appearing in Eq. (2.25) and the exponential appearing in Eq. (2.29), are due to the complex turning point. These terms are essentially singular for $c\to0$, but the exponential function vanishes rapidly for small (positive) c. The f term then becomes predominant, and one arrives at the very simple expression

$$|\mathscr{R}|^2=|\alpha_n c|^2, \tag{2.30}$$

valid for small c.

The function f accounts for the shape of the CAP (see Appendix A). This may be used to construct particular shapes that make the CAP reflection-free for a single energy.[18]

D. Optimal CAP parameters

With the approximate formulas obtained for the transmission and the reflection it is possible to derive optimal values for a as function of b. By optimal we mean that $|\mathscr{R}|^2+|\mathscr{T}|^2$ is minimal for given CAP length L and energy E. To this end one considers the derivative of $|\mathscr{R}|^2+|\mathscr{T}|^2$ that has to vanish for the optimal parameter $a_{\rm opt}$:

$$\frac{\partial}{\partial a}\{|\mathscr{R}|^2+|\mathscr{T}|^2\}|_{a=a_{\rm opt}}=0. \tag{2.31}$$

Using the high energy approximations (2.16) and (2.30) the criterion (2.31) gives the following equation for $a_{\rm opt}$:

$$\frac{2\alpha_n^2 a_{\rm opt}}{b^{2n}}=\frac{b}{n+1}\ \exp\left(-\frac{a_{\rm opt}b}{n+1}\right). \tag{2.32}$$

The relation (2.32) can be rewritten as

$$\frac{a_{\rm opt}b}{n+1}=2(n+1)\log(\gamma_n b)-\log\left[\frac{a_{\rm opt}b}{2(n+1)^2}\right], \tag{2.33}$$

where the parameter γ_n is defined by

$$\gamma_n:=[2(n+1)^{3/2}\alpha_n]^{-1/(n+1)}. \tag{2.34}$$

In particular one obtains: $\gamma_1=1.189$, $\gamma_2=0.9165$, $\gamma_3=0.7598$, and $\gamma_4=0.6536$. One iteration of Eq. (2.33) yields

$$a_{\rm opt}^0=\frac{2(n+1)^2}{b}\log(\gamma_n b)-\frac{n+1}{b}\log\log(\gamma_n b). \tag{2.35}$$

This formula works well for large b and yields a convenient starting point for more accurate calculations. To obtain these more accurate approximations we have to use a better approximation for $\mathscr{R}$, i.e., Eq. (2.29). Furthermore we approximate

$$\frac{d}{da}|\mathscr{R}|^2\approx\frac{2}{a}|\mathscr{R}|^2 \tag{2.36}$$

and

$$g'(a)\approx\frac{g(a)}{a}. \tag{2.37}$$

Now applying the condition (2.31) to Eq. (2.13) yields

$$g(a_{\rm opt})=\frac{n+1}{b}\log\left(\frac{g(a_{\rm opt}^0)b}{2|\mathscr{R}|^2(n+1)}\right), \tag{2.38}$$

where $|\mathscr{R}|^2$ is given by Eq. (2.29) and is evaluated at $c=a_{\rm opt}^0(b)/b^n$. After evaluation of the right-hand side, one uses Eq. (2.19) to determine $a_{\rm opt}$. Equation (2.38) yields an excellent approximation (except for the interference region, see below), as the comparison to numerically minimized reflection and transmission demonstrates.

The reflection curve shows oscillations in the intermediate energy range (see below). Here, the dominance of the tangent term and the f term changes and when both terms are of comparable magnitude one observes a pronounced interference structure in the reflection curve. If one is only interested in an upper limit for the reflection, one can make the curve monotonic by setting the relative phase to 1. Thus one obtains an alternative formula to Eq. (2.29) which reads

$$|\mathscr{R}_M|^2=\left\{\frac{\left|\frac{f(c)-1}{f(c)+1}\right|+\exp\left[-2\sin\left(\frac{\pi}{2n}\right)\beta_n c^{-1/n}\right]}{1+\left|\frac{f(c)-1}{f(c)+1}\right|\exp\left[-2\sin\left(\frac{\pi}{2n}\right)\beta_n c^{-1/n}\right]}\right\}^2. \tag{2.39}$$

By construction, this approximation to the reflection increases monotonically with c. It avoids the cusps in the $a_{\rm opt}(b)$ curve (see below) caused by the multiple minima but still yields almost the correct values for $a_{\rm opt}$, except for the interference region.

Often, one is interested in parameters which allow simultaneous optimization over an energy range $[E_1,E_2]$. Here, the monotonic approximation to the reflection becomes important. Since $|\mathscr{R}_M|^2$ monotonically decreases, whereas $|\mathscr{T}|^2$ monotonically increases with E, an optimal choice of the parameters is given if

$$|\mathscr{R}_M(E_1)|^2=|\mathscr{T}(E_2)|^2. \tag{2.40}$$

Since we now consider two energies simultaneously, two sets of parameters appear which are related to each other (for fixed η and L) by

$$\frac{a_1}{a_2}=\frac{E_2}{E_1},\quad \frac{b_1}{b_2}=\left(\frac{E_1}{E_2}\right)^{1/2},\quad \frac{c_1}{c_2}=\left(\frac{E_2}{E_1}\right)^{(2+n)/2}. \tag{2.41}$$

Let us begin with the simplest case and adopt Eqs. (2.16) and (2.30) to represent $\mathscr{T}$ and $\mathscr{R}$, respectively. Equations (2.40) and (2.41) then yield

$$|\alpha_n|^2\frac{a_2^2}{b_2^{2n}}\left(\frac{E_2}{E_1}\right)^{2+n}=\exp\left(-\frac{a_2b_2}{n+1}\right). \tag{2.42}$$

By a series of transformations, similar to those above, one obtains

$$a_{2,\rm opt}^0=\frac{2(n+1)^2}{b_2}\log\left[\tilde{\gamma}_n\left(\frac{E_1}{E_2}\right)^{(2+n)/(2+2n)}b_2\right]-\frac{2(n+1)}{b_2}\log\log\left[\tilde{\gamma}_n\left(\frac{E_1}{E_2}\right)^{(2+n)/(2+2n)}b_2\right], \tag{2.43}$$

where

$$\tilde{\gamma}_n=[2(n+1)^2|\alpha_n|]^{-1/(n+1)}, \tag{2.44}$$

i.e., $\tilde{\gamma}_1=1$, $\tilde{\gamma}_2=0.7631$, $\tilde{\gamma}_3=0.6389$, and $\tilde{\gamma}_4=0.5564$.

Equation (2.43) may be improved by adopting now Eqs. (2.13) and (2.39) to represent $\mathscr{T}$ and $\mathscr{R}$, respectively. This yields

$$g(a_{2,\mathrm{opt}}) = -\frac{n+1}{b_2}\log|\mathscr{R}_M|^2, \tag{2.45}$$

where $\mathscr{R}_M$ is evaluated at

$$c := \frac{a_{2,\mathrm{opt}}^0}{b_2^n}\left(\frac{E_2}{E_1}\right)^{(2+n)/2}. \tag{2.46}$$

If we want to determine optimal parameters to keep reflection and transmission below a certain limit (see below) the procedure is different. Let us regard an energy interval $[E_1, E_2]$ and a certain limit. In a first step, one has to determine an optimal value c_{opt} that yields a reflection (2.39) below this limit. Using Eqs. (2.8) and (2.41) with the parameter c_{opt} one then may express the transmission (2.13) as a function of b_2 only. Setting $|\mathscr{T}|^2$ to the desired limit one obtains an equation for b_2. This yields the complete set of optimal parameters.

III. NUMERICAL METHOD

In order to calculate the reflection and the transmission of the CAP in an efficient way we treated the CAP as a scattering potential and determined the scattering into the reflection and the transmission channel, respectively. Thus we have to examine the scattering off an one-dimensional CAP W_{scat} of finite length and in this way it is possible to apply wave packet methods.

To perform an energy resolved analysis of reflection and transmission we applied a time-to-energy Fourier transformation[22,23] to the solution $\psi(t,x)$ of the time-dependent Schrödinger equation. In order to obtain incoming eigenstates $\psi_E^+(x)$ to the real energy E, we chose a purely incoming initial wave packet $\psi(t=0,x)$. The eigenstates $\psi_E^+(x)$ can then be constructed according to

$$\psi_E^+(x) = \frac{1}{2\pi\Delta(E)}\lim_{\epsilon\to+0}\int_{-\infty}^{+\infty} e^{iEt-\epsilon t^2}\psi(t,x)\,dt. \tag{3.1}$$

We require that ψ_E^+ is energy normalized, i.e.,

$$\langle\psi_E^+|\psi_{E'}^+\rangle = \delta(E-E'). \tag{3.2}$$

This determines $\Delta(E)$ as

$$|\Delta(E)|^2 = \langle\psi(0)|\,\delta(H-E)\,|\psi(0)\rangle. \tag{3.3}$$

When the initial wave packet $\psi(0)$ is localized in the region where the potential has vanished, the coefficients $\Delta(E)$ are given by Fourier transformation of the initial wave packet:

$$\Delta(E) = \sqrt{\frac{m}{2\pi k}}\int_{-\infty}^{+\infty}\psi(t=0,x)e^{ikx}\,dx, \tag{3.4}$$

with $k=\sqrt{2mE/\hbar^2}$.

The transmission coefficient $\mathscr{T}$ and the reflection coefficient $\mathscr{R}$ can be determined from the asymptotic behavior of the energy normalized scattering wave function

$$\psi_E^+(x) \xrightarrow{x\to+\infty} \sqrt{\frac{m}{2\pi k}}\mathscr{T}e^{-ikx} \tag{3.5}$$

and

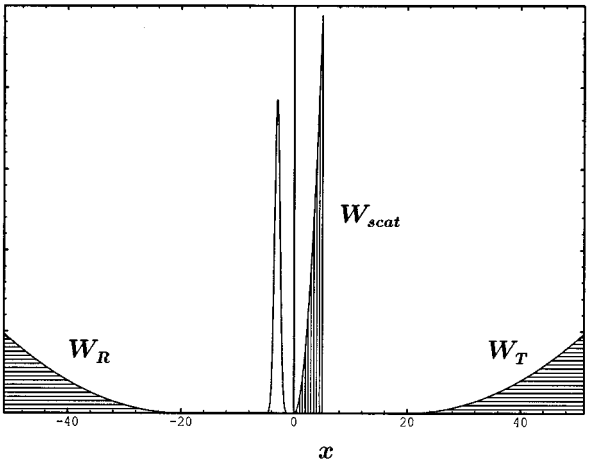

FIG. 1. Arrangement of the initial wave packet, the scattering CAP W_{scat}, which is to be examined, and the boundary CAPs W^R and W^T, which are used to determine the reflection and transmission, respectively.

$$\psi_E^+(x) \xrightarrow{x\to-\infty} \sqrt{\frac{m}{2\pi k}}\{e^{-ikx} + \mathscr{R}e^{ikx}\}, \tag{3.6}$$

respectively. In order to calculate $|\mathscr{R}|^2$ and $|\mathscr{T}|^2$, we investigate the flux[2] outside the interval where the CAP W_{scat} is located. To this end, we introduce the flux operator F^γ for the two different arrangement channels $\gamma = R, T$

$$F^\gamma := \frac{1}{m}\left[\delta(x-x_\gamma)\frac{1}{i}\frac{\partial}{\partial x} + \frac{1}{i}\frac{\partial}{\partial x}\delta(x-x_\gamma)\right]. \tag{3.7}$$

Here, the point x_γ describes a ''surface'' with respect to which the flux is determined. According to the arrangement presented in Fig. 1, the points x_γ are positioned at $x_R = -20.0$ for the reflection channel and at $x_T = 20.0$ for the transmission channel. Then the connection between reflection, transmission and flux is given by

$$2\pi\langle\psi_E^+|F^\gamma|\psi_E^+\rangle = \begin{cases} |\mathscr{R}|^2: & \gamma = R \\ |\mathscr{T}|^2: & \gamma = T \end{cases}. \tag{3.8}$$

In order to determine the flux into the different channels γ we used two additional CAPs, called W^R and W^T, located in the arrangement channels $\gamma = R$ and $\gamma = T$, respectively. By means of these boundary CAPs W^γ it is possible to compute the flux directly. The details of the formalism used are to be published elsewhere.[12] The resulting working equation reads

$$2\pi^2|\Delta(E)|^2\langle\psi_E^+|F^\gamma|\psi_E^+\rangle = \int_0^{+\infty}dt\int_0^{+\infty}dt'\; e^{-iE(t-t')} \times\langle\psi(t)|W^\gamma|\psi(t')\rangle. \tag{3.9}$$

In order to avoid the performance of the double integral, we determine the auxiliary wave functions

$$\psi_{E\gamma}^W = \int_0^{+\infty}dt\; e^{iEt}(W^\gamma)^{1/2}\psi(t) \tag{3.10}$$

by FFT and compute the flux by evaluation of the scalar product

$$\langle \psi_E^+ | F^\gamma | \psi_E^+ \rangle = \langle \psi_{E\gamma}^W | \psi_{E\gamma}^W \rangle. \tag{3.11}$$

Equation (3.9) is exact as long as the boundary CAPs W^γ can be considered as nonreflecting.

For the representation of the wave function and the Hamiltonian, we used an equidistant one-dimensional grid of 4096 points for the interval $[-51.2,51.2]$ with a grid spacing $\Delta x = 0.025$. Dimensionless coordinates, mass $m=1$, and $\hbar = 1$ are employed throughout. Due to the scaling properties (2.3), (2.5), and (2.8) one can easily transform the obtained results to any particular case. The scattering CAP W_{scat} starts at $x=0$ and ends at $x=L$. In the approximate formulas (2.13) and (2.16) for $|\mathscr{T}|^2$, we used the length $L' = L + \Delta x/2$ to adjust for the ambiguity caused by the finite grid spacing. The CAPs W^γ applied to determine the flux in the arrangement channel γ are of quartic type and located on the intervals $[-51.2,-20.0]$ for $\gamma = R$ and $[20.0,51.2]$ for $\gamma = T$, respectively. This rather long absorption distance allows a small CAP strength $\eta = 10^{-4}$ for W^γ, such that reflections at W^γ could be supposed to be negligible. We used a free propagating wave packet to make sure that this assumption was sufficiently fulfilled. The arrangement of the different CAPs is sketched in Fig. 1.

The kinetic energy operation was accomplished by the Fourier method.[24] The propagation of the wave packet was performed by means of the pseudo-spectral Newton propagation method.[13–15] This method appears to be rather stable for the propagation with complex Hamiltonians. In contrast to other methods, the Newton propagation avoids the calculation of c-products,[25] which appear to be the main source of instabilities.

The initial wave packet is given by

$$\psi(x) = \left(\frac{\alpha}{2\pi}\right)^{1/4} e^{-\alpha(x-x_0)^2 - ip_0 x}, \tag{3.12}$$

where x_0 is the initial spatial center, p_0 the initial momentum of the wave packet, and α determines its spatial width. In order to exclude artefacts due to the choice of parameters, we tried different values for p_0 and α. However, p_0^2/α was chosen large enough to reduce the backward moving parts of the wave packet to a negligible amount. The center x_0 was selected in such a way that the initial overlap between the wave packet and the CAP was negligibly small.

IV. RESULTS

We shall only discuss the numerical results for the quadratic and the quartic CAP. For other orders the results are similar.

In Fig. 2, the numerical energy resolved reflections for a quadratic CAP are compared to the results obtained by Eqs. (2.29) and (2.30). The three triples of curves are computed for different CAP lengths ($L = 1.0,\ 2.5,\ 6.25$) where different adapted parameters ($\eta = 320,\ 26.6,\ 2.16$) are used for every L, respectively. The parameters are chosen in such a way, that the sum of transmission and reflection becomes

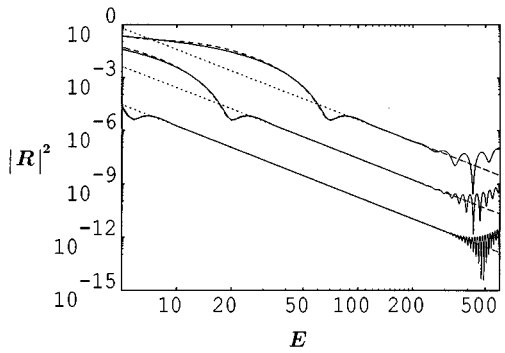

FIG. 2. Reflection as a function of the energy E for the quadratic CAP $-i\eta x^2$ for different parameters. The first set of curves from above belongs to the parameters $L=1.0$ and $\eta=320$, the next one to $L=2.5$ and $\eta=26.6$, and the last one to $L=6.25$ and $\eta=2.16$. The solid lines represent the numerical results, the dotted lines the linear approximations (2.30) and the dashed lines to the results obtained with Eq. (2.29) where $c=\eta/(2E^2)$.

minimal for energies between $E=80$ and $E=100$. For each of the three CAP lengths, one observes, that for an intermediate energy range the behavior of the numerical curve is linear in the double logarithmic plot. Here the simple approximation (2.30), indicated by the dotted line, becomes essentially exact. This intermediate regime becomes larger with growing L. For higher energies ($E>250$) one observes oscillations which are due to the finite length of the CAP. These move to still higher energies if one enlarges L and holds η and n constant. These oscillations are of minor importance since the transmission is predominant at these energies.

For small energies one observes a deviation from the linearity, and only the full approximation (dashed line) given by Eq. (2.29) can reproduce the correct behavior. Residual differences may be due to the neglection of higher order terms in f. For the quadratic CAP we tested the quality of the numerical procedure by comparison to the exact reflection formula given by Eqs. (2.23) and (2.24). We obtained a complete agreement between the two curves and so the correctness of the numerical procedure is justified.

In Fig. 3, similar curves to those in Fig. 2 are presented for quartic CAPs. Here the same CAP lengths are used, but different adapted parameters ($\eta = 392,\ 9.44,\ 0.140$) were selected in a way similar as above. The behavior corresponds to that of the quadratic CAP, but the deviation from linearity for low energies becomes even more pronounced, since the turning point moves closer to the real axis with increasing order n. We have no exact analytic results for the reflection of quartic CAPs, but Eq. (2.29) also seems to yield an almost exact description in this case. Calculations for the linear and cubic CAP yield a similar agreement between the numerical results and the prediction (2.29).

In Fig. 4, the corresponding numerical results for the transmission of a quadratic CAP using the same parameters as for the reflection are represented. The simple approximation (2.16), describes the transmission in the high energy limit, but for lower energies this approximation is disastrous.

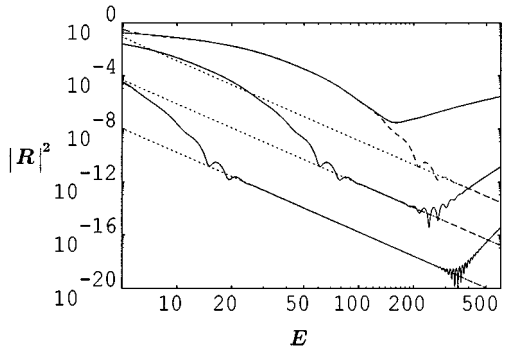

FIG. 3. Reflection as a function of the energy E for the quartic CAP $-i\eta x^4$ for different parameters. The first set of curves from above belongs to the parameters $L=1.0$ and $\eta=392$, the next one to $L=2.5$ and $\eta=9.44$, and the last one to $L=6.25$ and $\eta=0.140$. The curves are calculated in the same way as for Fig. 2 but $c=\eta/(4E^3)$.

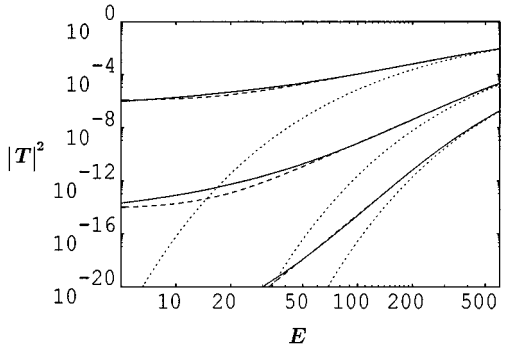

FIG. 5. Transmission as a function of the energy E for the quartic CAP $-i\eta x^4$ for the same parameters as for Fig. 3. The various line types are the same as in Fig. 4.

Here the approximation (2.18) for $g(a)$, becomes important and this yields satisfactory results over the entire energy range. The differences are somewhat larger than for the reflection (if one ignores the effects of the finite length L) but, nevertheless, the description is quite good. If one is interested in a very accurate representation one may evaluate the integral in Eq. (2.11) numerically, yielding an excellent agreement with the numerically exact calculation (no differences visible on the plot).

The results for the quartic CAP, presented in Fig. 5, show more or less the same behavior. If one compares the results of quadratic and quartic CAPs, one observes that for $L=1.0$ the quadratic CAP yields a better absorption than the quartic CAP, while the situation for $L=6.25$ is reversed. The question of the optimal choice for the order n is treated in the following in more detail.

In Fig. 6, the numerically optimized parameters a_{opt} are presented as a function of b. The solid line is calculated using the complete approximations (2.13) and (2.29), while the dashed line is obtained for the monotonic reflection (2.39). While the curve calculated for the monotonic reflection is rather smooth, the curve using the full approximation shows leaps in the parameter a_{opt}. The number of these leaps increases with growing n. The curve calculated with the monotonic estimate of the reflection $\mathscr{R}_M$ does not show such leaps since here the minimum is unambiguous. However, except for the region of interference the two curves are almost identical. A characteristic point is that the parameter a must be chosen larger as the order n becomes higher. For every curve one has essentially to distinguish two b ranges. For large b values one finds a linear behavior for a_{opt}, which corresponds to the linear behavior of the reflection for high energies [see Eq. (2.30)]. At small b values (ignoring the leaps of the solid curve) one finds an almost stationary behavior of the parameter a.

In Fig. 7, the numerically optimized values of $|\mathscr{R}|^2+|\mathscr{T}|^2$ as functions of b are represented. While the solid curve is obtained by numerical minimization of $|\mathscr{R}|^2+|\mathscr{T}|^2$ evaluated with the approximations (2.13) and (2.29) (i.e., employing the a_{opt} values of Fig. 6), the dotted curve is obtained using a values calculated with Eq. (2.38). The parameters a_{opt} obtained by Eq. (2.38) are very accurate

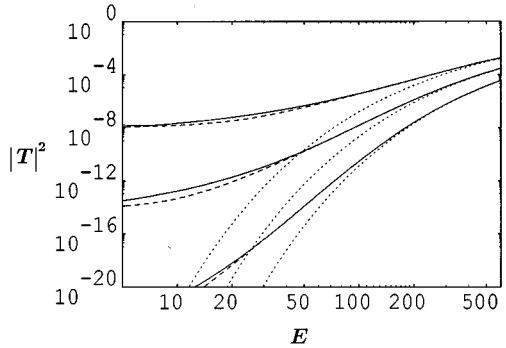

FIG. 4. Transmission as a function of energy E for the quadratic CAP $-i\eta x^2$ for different sets of parameters, which are the same as for Fig. 2. The solid lines represent the numerical results, the dotted lines the linear approximation due to Eq. (2.16), and the dashed lines the results obtained with Eqs. (2.13) and (2.18).

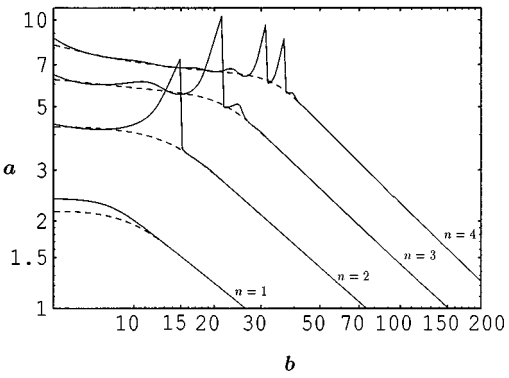

FIG. 6. Optimized parameters a_{opt} as a function of b for different monomial CAPs $-i\eta x^n$, $(n=1,2,3,4)$. The parameters a_{opt} are determined by numerically minimizing $|\mathscr{R}|^2+|\mathscr{T}|^2$. For the solid line the full approximation (2.29) is applied, while for the dotted line the monotonic reflection estimate (2.39) is used. Since $b=kL$ and $\eta=aEL^{-n}$ one may use this graph to determine the optimal CAP strength η for a given absorption length L and scattering energy E.

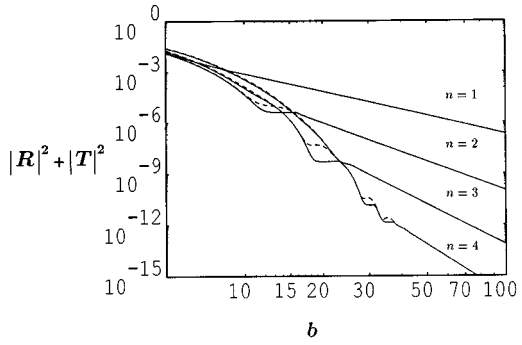

FIG. 7. Optimized values of $|\mathscr{R}|^2+|\mathscr{T}|^2$ as a function of b for different monomial CAPs $-i\eta x^n$, $(n=1,2,3,4)$. The parameter a was determined by numerically minimizing $|\mathscr{R}|^2+|T|^2$ (solid line) or by using a_{opt} as defined by Eq. (2.38) (dotted line). Except for the interference region, Eq. (2.38) yields quite accurate a_{opt} parameters. Note that the solid lines of Figs. 6 and 7 correspond to each other.

except for the interference region where the curves show plateaus. If we regard the general behavior of the curves, we find similar features to those observed by Vibók and Balint-Kurti.[9] However, the particular values of $|\mathscr{R}|^2+|\mathscr{T}|^2$ differ in some cases by two orders of magnitude. We will return to this point later. As a general rule, we note, that the optimal order n increases with increasing b, as exhibited by Figs. 2–5.

Similar results to those in Fig. 7, are obtained from Table I. One finds that the b values increase with the required accuracy. Again, higher CAP orders are preferable for more accurate calculations. Comparing in particular the results for the errors $|\mathscr{R}|^2+|\mathscr{T}|^2$ of 10^{-6}, 10^{-9}, and 10^{-12}, one observes that the higher order CAP needs a smaller b, i.e., a smaller CAP length. The corresponding a values increase as well, but not so rapidly as the b values. Thus the optimal a values are about 4 for the quadratic CAP, about 5 for the cubic CAP, and about 6 for the quartic CAP. Moreover, in Table I the optimal parameters a and b for the monotonic reflection formula (2.39) are compared to those

TABLE I. Numerically optimized parameters for monomial CAP with respect to a given limit for $|\mathscr{T}|^2+|\mathscr{R}|^2$, called ''error'' in the following. n denotes the order of the CAP. Optimal n values are marked with a star. b_{opt} is the minimal b value and a_{opt} the optimal a value, which are to be chosen such that $|\mathscr{T}|^2+|\mathscr{R}|^2$ remains below the error limit. The values with the upper index 1 are obtained by using the monotonic reflection approximation (2.39) while the values with the upper index 2 are obtained by using the reflection approximation (2.29), respectively. We recommend the use of the former.

Error	n	$b_{\text{opt}}^{(1)}$	$a_{\text{opt}}^{(1)}$	$b_{\text{opt}}^{(2)}$	$a_{\text{opt}}^{(2)}$
10^{-2}	2*	5.3	4.25	5.3	4.31
10^{-3}	2*	7.5	4.20	7.5	4.17
10^{-4}	2*	9.5	4.09	9.5	4.28
10^{-5}	2*	13.2	3.76	11.2	4.60
10^{-6}	2	19.9	2.92	19.9	2.93
10^{-6}	3*	15.7	5.55	15.3	5.54
10^{-7}	3*	18.8	5.34	18.1	6.42
10^{-8}	3*	22.8	4.95	22.2	4.98
10^{-9}	3	29.6	4.10	29.6	4.12
10^{-9}	4*	25.6	6.48	25.5	6.41
10^{-10}	4*	28.8	6.35	27.4	6.52
10^{-11}	4*	32.7	6.01	32.0	6.04
10^{-12}	4	38.9	5.48	38.2	5.59
10^{-12}	5*	37.6	7.14	37.2	7.24

obtained by application of Eq. (2.29). Using Eq. (2.39), the reflection is overestimated such that larger or at least equal b values are required.

In Table II, optimal parameters for energy intervals $[E_1,E_2]$ are compiled. Here, the determining parameter is the quotient E_1/E_2. Compared to the results of Table I, equal or higher CAP orders are found to be optimal. In particular, the third order CAP yields an optimal choice over a large scale of error limits. Moreover, larger b values are needed to obtain the same error limits. This is obvious, since the error limit must hold for the entire energy range $[E_1,E_2]$. Thus, the larger the chosen energy range the larger the required b values become. At the same time the optimal a values become smaller for larger energy ranges. It is inter-

TABLE II. Numerically optimized parameters for monomial CAP with respect to a given limit for $|\mathscr{T}|^2+|\mathscr{R}|^2$, called ''error'' in the following. Here the parameters are optimized with respect to an energy range $[E_1,E_2]$. The optimal values depend on the quotient E_1/E_2. The parameters are optimized for three different quotients $E_1/E_2=1/3$, $E_1/E_2=1/10$, and $E_1/E_2=1/30$. $c_{1,\text{opt}}^{(n)}$ denotes an optimal c value for a monomial CAP of order n. n_{opt} denotes the optimal CAP order. $b_{2,\text{opt}}$ and $a_{2,\text{opt}}$ denote the optimal parameters (with respect to E_2) yielding a transmission below the error limit. All values are obtained by application of the monotonic reflection formula (2.39).

				$E_1/E_2=1/3$			$E_1/E_2=1/10$			$E_1/E_2=1/30$		
Error	$c_{1,\text{opt}}^{(2)}$	$c_{1,\text{opt}}^{(3)}$	$c_{1,\text{opt}}^{(4)}$	n_{opt}	$b_{2,\text{opt}}$	$a_{2,\text{opt}}$	n_{opt}	$b_{2,\text{opt}}$	$a_{2,\text{opt}}$	n_{opt}	$b_{2,\text{opt}}$	$a_{2,\text{opt}}$
10^{-2}	1.8×10^{-1}	4.3×10^{-2}	6.8×10^{-3}	2	9.2	1.69	3	19.4	0.99	3	41.2	0.61
10^{-3}	8.3×10^{-2}	1.3×10^{-2}	1.3×10^{-3}	2	11.7	1.26	3	29.0	1.00	3	57.1	0.49
10^{-4}	4.2×10^{-2}	5.6×10^{-3}	4.3×10^{-4}	2	16.9	1.33	3	38.4	1.00	3	75.7	0.49
10^{-5}	2.1×10^{-2}	2.8×10^{-3}	1.7×10^{-4}	3	23.4	2.30	3	48.3	1.00	3	95.2	0.49
10^{-6}	7.9×10^{-3}	1.5×10^{-3}	8.6×10^{-5}	3	28.5	2.23	3	59.1	0.98	3	116.5	0.48
10^{-7}	2.5×10^{-3}	8.7×10^{-4}	4.6×10^{-5}	3	34.2	2.23	3	70.3	0.96	3	138.7	0.47
10^{-8}	8.0×10^{-4}	4.4×10^{-4}	1.6×10^{-5}	3	41.5	2.02	3	86.1	0.89	3	169.9	0.44
10^{-9}	2.5×10^{-4}	1.6×10^{-4}	9.7×10^{-6}	4	50.7	2.37	4	102.3	1.06	4	196.4	0.53
10^{-10}	8.0×10^{-5}	5.3×10^{-5}	5.5×10^{-6}	4	52.0	1.49	4	117.0	1.03	4	224.7	0.52

esting to note, that the optimal a (b) values for $E_1/E_2=1/10$ are nearly half (double) the size as for $E_1/E_2=1/30$. In the limit of wide energy ranges, one finds almost identical a values to be optimal for all error limits: approximately 1 for $E_1/E_2=1/10$ and 0.5 for $E_1/E_2=1/30$, independent of b_{opt}.

V. DISCUSSION

In this paper, we developed approximate representations of CAP reflection and transmission. In particular, we concentrated on the case of monomial CAPs, since firstly they allow simple scaling rules, and secondly they present the CAP type most widely used in practical work. While the approximation of the transmission is quite straightforward, the problem of describing the reflection is more difficult. Here we could identify two effects determining the principle behavior of the reflection, which both could be described by WKB procedures. The structure of our approximations agrees with the exact analytical results that we obtained for the quadratic CAP in an earlier work.[17] It is possible to transfer the structure of the reflection for the quadratic CAP to all orders n. Based on this structure, we obtained approximations of astonishing quality. In fact, it is likely that the form (2.29) describes the actual structure of reflection for all monomial CAPs.

This excellent description of the reflection allows the application of the obtained formulas to optimize the CAP parameters. Such representations are important tools to find properly adapted CAPs for every particular problem. On the other hand, such representations reveal the major features of CAPs and thus increase one's understanding of the nature of CAP reflection and transmission. This is of importance for the creation of new types of CAPs.

Surprisingly, our numerical results for minimized values of reflection and transmission do not agree with those of Vibók and Balint-Kurti.[9] We obtain optimal reflections and transmissions which in some cases differ by two orders of magnitude from those in Ref. 9. On the other hand, the results for the values of a_{opt} are similar. Further differences appear in the description of the asymptotic behavior of $a_{\mathrm{opt}}(b)$ for large b values. While our results show uniform spacings between the different CAP orders (see Fig. 7) the results of Vibók and Balint-Kurti show a very small difference between the quadratic and the cubic CAP. From the theoretical point of view as developed in Sec. II we do not see any reasons for the latter behavior. By comparison, to the exact analytical results, it is certain that our numerical results are correct for the quadratic CAP at least. Moreover, the WKB approximation valid for all CAP orders agrees so well with our numerical results, that we see no reasons to doubt the correctness of either of these.

At this point it is to be remarked, that the present investigation only deals with an important but limited class of CAPs. Another question is the search for optimal forms of CAPs. Here, in particular, the efforts to construct reflection-free, or perfect, absorbing potentials are to be mentioned. Such perfect absorbers profit from interference effects analogous to those observed in Figs. 2 and 3. By constructing CAPs of more complicated forms this interference can be made completely destructive leading to zero reflection at a certain energy. In this regard, we want to refer the reader to other works,[10,18,27] where this point is studied in more detail.

Returning to Fig. 7 and Table I, we emphasize again that the order n of the CAP should be chosen the larger the higher the required accuracy. For example, for an error limit of 10^{-12} a CAP of order 5 is optimal. This demonstrates that the chosen order should not be too small. Concentrating on a single energy we found the following relations:

$$\begin{aligned} b<16 \quad &: \quad n=2, \\ 16\leqslant b<26 \quad &: \quad n=3, \\ 26\leqslant b \quad &: \quad n\geqslant 4, \end{aligned} \tag{5.1}$$

to be useful. In order to optimize a CAP over an energy interval, consult Table II. Finally, we note, that a CAP of order $n=1$ is never an optimal choice.

ACKNOWLEDGMENTS

The authors thank G. Worth for critically reading the manuscript. Financial support by the Deutsche Forschungsgemeinschaft is gratefully acknowledged.

APPENDIX A

In this Appendix, we calculate the logarithmic derivative $\mathscr{C}(c)$, which determines the reflection coefficient $\mathscr{R}$. We show that $\mathscr{C}(c)$ is a product of a tangent term and a function f [see Eq. (2.23)] and determine f up to first order in c, i.e., we derive the coefficients α_n. The tangent term is essentially singular, and hence, cannot be expanded in powers of c. We show that the tangent term originates from a complex turning point.

We shall use a WKB ansatz to derive the proposed results. In order to account for the complex turning point we make use of the Airy uniform WKB approximation[21] and define

$$\psi_0(\zeta) := Q'^{-1/2} z^{1/4}\ \mathrm{Ai}(-z), \tag{A1}$$

where

$$z := (\tfrac{3}{2}Q)^{2/3} \tag{A2}$$

and

$$Q(\zeta) := \int_{\zeta}^{\zeta_t} \sqrt{1+ics^n}\, ds. \tag{A3}$$

Here $\zeta_t := (i/c)^{1/n}$ denotes the turning point.

Differentiating the ansatz (A1) twice one finds

$$\psi_0'' + Q'^2\psi_0 = \left\{ \frac{3}{4}\left(\frac{Q''}{Q'}\right)^2 - \frac{1}{2}\frac{Q'''}{Q'} - \frac{5}{36}\left(\frac{Q'}{Q}\right)^2 \right\}\psi_0. \tag{A4}$$

The left-hand side of the equation above is just the Schrödinger equation and the right-hand side is thus the error term.

Using a linear CAP (i.e., $n=1$) one finds $Q(\zeta)=(2i/3c)(1+ic\zeta)^{3/2}$ and the error term vanishes. In

this case ψ_0 is the exact solution. Employing an asymptotic form of the Airy function[19] one may expand [for $|Q|\to\infty$ and $\mathrm{Re}(Q)\geqslant 0$]

$$\mathrm{Ai}(-z)=\pi^{1/2}z^{-1/4}\sin\left[Q+\frac{\pi}{4}-\frac{5}{72}Q^{-1}+\frac{1105}{31104}Q^{-3}+\mathcal{O}(Q^{-5})\right]\times\left[1-\frac{5}{144}Q^{-2}+\frac{2285}{41472}Q^{-4}+\mathcal{O}(Q^{-6})\right]. \tag{A5}$$

Using this expansion to represent the wave function (A1) and taking the logarithmic derivative one arrives at

$$\frac{\psi_0'}{\psi_0}=-\frac{Q''}{2Q'}+Q'\cot\left[Q+\frac{\pi}{4}-\frac{5}{72}Q^{-1}+\frac{1105}{31104}Q^{-3}+\mathcal{O}(Q^{-5})\right]\left[1-\frac{5}{72}Q^{-2}+\frac{385}{3456}Q^{-4}+\mathcal{O}(Q^{-6})\right]^{-1}-\frac{5}{72}Q^{-3}+\frac{565}{2592}Q^{-5}-\mathcal{O}(Q^{-7}). \tag{A6}$$

To evaluate the logarithmic derivative at $\zeta=0$, one has to calculate $Q_0:=Q(0)$. Fortunately, this integral can be done for all n,

$$Q_0=\beta_n(i/c)^{1/n}, \tag{A7}$$

where

$$\beta_n=\frac{\Gamma(1+1/n)\Gamma(3/2)}{\Gamma(3/2+1/n)}. \tag{A8}$$

Note further that $Q'(0)=-1$, $Q''(0)=-(ic/2)\delta_{n,1}$ and $Q'''(0)=-ic\,\delta_{n,2}-(c^2/4)\delta_{n,1}$ holds.

For $n=1$, when ψ_0 becomes exact, we obtain

$$\measuredangle(c)=i\frac{\psi_0}{\psi_0'}(0)=-i\tan\left(Q_0+\frac{\pi}{4}\right)\left[1+\frac{c}{4}+\mathcal{O}(c^2)\right], \tag{A9}$$

where we have used $Q_0^{-1}\propto c$ (valid for $n=1$) and $|\sin[Q_0+(\pi/4)]|^2>c^{-1}$ which is valid since Q_0 is complex.

Comparing Eq. (A9) with Eqs. (2.25) and (2.26) one finds

$$\alpha_1=1/8. \tag{A10}$$

For $n>1$, however, the reciprocal of the logarithmic derivative of ψ_0 does not give $\measuredangle(c)$ correctly up to $\mathcal{O}(c^2)$. This is because the right-hand side of Eq. (A4) now contains terms which are of order c or even $c^{2/n}$. Thus, the wave function ψ_0 contains errors of these orders and one has to seek for a better approximation to the exact wave function ψ.

To arrive at such better approximations, one may resort to the higher order WKB formulas. Let Φ denote the exact phase integral, i.e., Eq. (A1) yields the exact wave function if Q is replaced by Φ in Eqs. (A1) and (A2). According to Eq. (A4), Φ must satisfy the differential equation

$$\Phi'^2=Q'^2+D(\Phi), \tag{A11}$$

where

$$D(\Phi)=\frac{3}{4}\left(\frac{\Phi''}{\Phi'}\right)^2-\frac{1}{2}\frac{\Phi'''}{\Phi'}-\frac{5}{36}\left(\frac{\Phi'}{\Phi}\right)^2. \tag{A12}$$

To satisfy $\psi(\zeta)\to 0$ for $\zeta\to\infty$, we assume $\Phi(\zeta)/Q(\zeta)\to 1$ for $\zeta\to\infty$ as boundary condition for Eq. (A11).

The differential Eq. (A11) may be solved by iteration. Developing the square root one obtains a first order approximation

$$\Phi(\zeta)=Q(\zeta)-\int_\zeta^\infty[2Q'(s)]^{-1}D[Q(s)]ds. \tag{A13}$$

The integral can be done, except for a term quadratic in c. Discarding this term one arrives at

$$\Phi=Q+\frac{5}{72}Q^{-1}-\frac{1}{4}\frac{Q''}{Q'^2}. \tag{A14}$$

Assuming $n=2$ one finds

$$\Phi(0)=Q_0+\frac{5}{72}Q_0^{-1}, \tag{A15a}$$

$$\Phi'(0)=-1+\frac{5}{72}Q_0^{-2}+\frac{ic}{4}, \tag{A15b}$$

$$\Phi''(0)=\frac{5}{36}Q_0^{-3}. \tag{A15c}$$

Hence all additional reciprocal Q_0 terms appearing in Eq. (A6) cancel to the desired order and we obtain (note $Q_0^2\propto c^{-1}$ for the case $n=2$ under consideration):

$$\measuredangle(c)=-i\tan\left(Q_0+\frac{\pi}{4}\right)\left[1+\frac{ic}{4}+\mathcal{O}(c^2)\right], \tag{A16}$$

i.e.,

$$\alpha_2=i/8. \tag{A17}$$

It is interesting to note, that the $(\Phi'/\Phi)^2$ term appearing in $D(\Phi)$ has the effect that all the additional reciprocal Q_0 terms cancel. The $(3/4)(\Phi''/\Phi')^2-(1/2)(\Phi'''/\Phi')$ term on the other hand, makes $\Phi'(0)$ become $-f(c)^{-1}$ (except for reciprocal Q_0 terms, see above).

To derive $\measuredangle(c)$ for the nth order monomial CAP one has to calculate the $(n-1)$th iterated phase integral. This is too cumbersome to do. Since we are now confident that the product for Eq. (2.25) is correct, it may be sufficient to determine the α_n by a method that ignores the complex turning point.

We modify the CAP by switching it off exponentially for large ζ. The wave function now becomes a free wave for $\zeta\to\infty$ and may be written as[26]

$$\psi(\zeta)=\mathrm{const}\cdot\exp\left[i\zeta-\int_\zeta^\infty h(s)ds\right]. \tag{A18}$$

Since ψ satisfies the Schrödinger equation

$$\psi''(\zeta)+(1+ic\zeta^n e^{-\lambda\zeta})\psi(\zeta)=0, \tag{A19}$$

one finds that h must satisfy the differential equation

$$h'=-2ih-h^2-ic\zeta^n e^{-\lambda\zeta}, \tag{A20}$$

subject to the boundary condition

$$\zeta h(\zeta)\to 0 \quad \text{for} \quad \zeta\to\infty. \tag{A21}$$

Setting

$$h=\sum_{j=1}^{\infty} c^j h_j \tag{A22}$$

and separating the orders one arrives at linear differential equations for the h_j, which can easily be solved

$$h_1(\zeta)=ie^{-2i\zeta}\int_{\zeta}^{\infty} s^n e^{-\lambda s}e^{2is}\,ds, \tag{A23a}$$

$$h_j(\zeta)=e^{-2i\zeta}\int_{\zeta}^{\infty} e^{-\lambda s}e^{2is}\sum_{l=1}^{j-1} h_l(s)h_{j-l}(s)ds. \tag{A23b}$$

Since

$$1+2\alpha_n c+\mathcal{O}(c^2)=i\frac{\psi(0)}{\psi'(0)}=[1-ih(0)]^{-1}$$
$$=1+ich_1(0)+\mathcal{O}(c^2), \tag{A24}$$

one finds

$$\alpha_n=\frac{i}{2}h_1(0)=-\frac{1}{2}\frac{n!}{(\lambda-2i)^{n+1}}. \tag{A25}$$

One now can perform the limit $\lambda\to 0$ and arrive at the desired result

$$\alpha_n=\frac{n!}{4i}\left(\frac{i}{2}\right)^n. \tag{A26}$$

By fitting Eq. (2.30) to the numerically obtained reflection coefficient, we independently determined the numbers α_n up to $n=4$ and found them in complete agreement with Eq. (A26).

[1] D. Neuhauser and M. Baer, J. Chem. Phys. **90**, 4351 (1989); **91**, 4651 (1989).
[2] D. Neuhauser, M. Baer, R. S. Judson, and D. J. Kouri, Comput. Phys. Comun. **63**, 460 (1991).
[3] R. Kosloff and D. Kosloff, J. Comput. Phys. **63**, 363 (1986).
[4] G. Jolicard and E. J. Austin, Chem. Phys. Lett. **121**, 106 (1985).
[5] D. Neuhauser and M. Baer, J. Phys. Chem. **94**, 185 (1990); J. Chem. Phys. **92**, 3419 (1990).
[6] T. Seideman and W. H. Miller, J. Chem. Phys. **97**, 2499 (1992).
[7] M. S. Child, Mol. Phys. **72**, 89 (1991).
[8] Á. Vibók and G. G. Balint-Kurti, J. Chem. Phys. **96**, 7615 (1992).
[9] Á. Vibók and G. G. Balint-Kurti, J. Phys. Chem. **96**, 8712 (1992).
[10] D. Macías, S. Brouard, and J. G. Muga, Chem. Phys. Lett. **228**, 672 (1994).
[11] T. Seideman and W. H. Miller, J. Chem. Phys. **96**, 4412 (1992).
[12] A. Jäckle and H.-D. Meyer, J. Chem. Phys. (submitted).
[13] M. Berman, R. Kosloff, and H. Tal-Ezer, J. Phys. A **25**, 1283 (1992).
[14] S. M. Auerbach and C. Leforestier, Comput. Phys. Commun. **78**, 55 (1993).
[15] R. Kosloff, Annu. Rev. Phys. Chem. **45**, 145 (1994).
[16] D. Kosloff and R. Kosloff, J. Comput. Phys. **52**, 35 (1983).
[17] U. V. Riss and H.-D. Meyer, J. Phys. B **26**, 4503 (1993).
[18] U. V. Riss and H.-D. Meyer, J. Phys. B **28**, 1475 (1995).
[19] M. Abramowitz and I. A. Stegun, *Handbook of Mathematical Functions* (Dover, New York, 1972).
[20] R. E. Langer, Phys. Rev. **51**, 669 (1937).
[21] M. S. Child, in *Dynamics of Molecular Collisions, Part B*, edited by W. H. Miller (Plenum, New York, 1976), pp. 171–215.
[22] E. J. Heller, J. Chem. Phys. **62**, 1544 (1975).
[23] D. J. Tannor and D. E. Weeks, J. Chem. Phys. **98**, 3884 (1993).
[24] R. Kosloff, J. Phys. Chem. **92**, 2087 (1988).
[25] N. Moiseyev, P. R. Certain, and F. Weinhold, Mol. Phys. **36**, 1613 (1978).
[26] H.-D. Meyer and O. Walter, J. Phys. B **15**, 3647 (1982).
[27] S. Brouard, D. Macías, and J. G. Muga, J. Phys. A **27**, L439 (1994).